ESTEEM Academic Journal
Vol. 13, June 2017, 1-17

A NOVEL ADSORBENT FORMED FROM BLAST FURNACE SLAG BY ALKALI FUSION FOR PHOSPHATE IONS REMOVAL

Takaaki Wajima[1*]

Department of Urban Environment Systems, Chiba University/1-33, Yayoi-cho, Inage-ku, Chiba, Japan

**Corresponding author: wajima@tu.chiba-u.ac.jp*

ARTICLE HISTORY

Received
1 January 2017

Received in revised form
15 March 2017

Accepted
30 March 2017

ABSTRACT

Blast furnace slag (BF slag) was converted using alkali fusion method into a novel adsorbent to remove phosphate from aqueous solutions. The slag was mixed with NaOH powder (NaOH / Slag = 1.6) and then heated at 600 °C for 6 h to prepare the fused precursor. The precursor was stirred in distilled water at room temperature to synthesize the adsorbent and its ability to remove phosphate from aqueous solution was investigated. F- and PO43- removal efficiencies by the adsorbent were higher than those of raw BF slag, with the removal of PO43- being particularly excellent (99%), while Cl-, SO42-, NO3- and Br- were barely adsorbed. With increasing pH of the solution to around pH 7, phosphate removal of the product increases, and then becomes almost constant. The equilibrium adsorption capacity of the product for PO43- was found to fit the Freundlich isotherm better than the Langmuir isotherm, and the calculated maximum PO43- adsorption capacity of the product was 7.67 mmol/g. Phosphate removal corresponded better to a pseudo second-order kinetic model than a pseudo first-order model. The high affinity of the adsorbent for PO43- in aqueous solution was caused by the formation of hydroxyapatite [Ca5(PO4)3(OH)] and brushite [CaHPO4•2H2O].

Keywords: blast burnace slag; alkali fusion; phosphate removal; high selectivity. hydrocalumite; hydroxyapatite; brushite

1. INTRODUCTION

Phosphate is usually considered as the limiting nutrient for the eutrophication of natural water bodies. Therefore, water treatment facilities remove phosphate from wastewater before it is returned to the environment. Various techniques have been used for phosphate removal, and chemical precipitation, adsorption, and biological methods have been applied successfully. Adsorption is a comparatively useful and efficient technique for removing phosphate from wastewater (Ugurlu & Salman, 1998).

p-ISSN 1675-7939; e-ISSN 2289-4934

For recycling and re-use of wastes with energy efficient, environmentally friendly and cost-effective phosphate adsorbents can be produced from many raw materials, such as industrial and agricultural wastes, at low cost. For example, coal fly ash (Can & Yildiz, 2006; Lu, et al., 2009), slag (Johansson & Gustafsson, 2000), red mud (Chang-jun, et al., 2007), alum sludge (Huang & Chiswell, 2000), cow bone (Hoon & Kang, 2002), peat (Xiong & Mahmood, 2010), oyster shell (Namasivayam, et al., 2005), scallop shell (Yeom & Jung, 2009), wheat straw (Xu, et al., 2010), and iron oxide tailings (Zeng, et al., 2004) have been used to remove phosphate.

Blast furnace slag (BF slag) is the largest by-product from pig iron metallurgical furnaces, with approximately 150 million metric tons of slag produced annually worldwide (Ozdemir & Yilmaz, 2007; Savastona, et al., 1999). In Japan, more than 25 million tons of BF slag is produced annually, which is widely used for cement production, road construction, and as a concrete aggregate. However, the demand for recycled BF slag for these applications has been saturated and the development of value-added products from BF slag has become an important issue for establishing a sustainable society (Fujiwara, 2003). Therefore, researches on various recycling processes have recently been carried out (Yabuta, et al., 2004; Lee, et al., 2003;. Miki, et al., 2004;. Kuroki, et al., 2007).

In my previous study, we converted BF slag into a hydroxide-based adsorbent, containing calcite and hydrocalumite, using alkali fusion, and confirmed that the adsorbent has high affinity for removing phosphate from aqueous solution (Wajima, et al., 2011). While this adsorbent is expected to be useful for removing phosphate from aqueous solution, more information is required on its properties before it can be widely applied.

In this study the conversion of the BF slag into a hydroxide adsorbent using alkali fusion was achieved, and the phosphate removal ability of the adsorbent was examined for wastewater treatment.

2.EXPERIMENTAL

2.1 Materials

BF slag can be divided into air- and water-cooled slag according to the cooling method. These slags contain crystalline and amorphous phases, respectively. The BF slag used in this study (received from one of the steel-making plants in Japan) was water-cooled. The BF slag was ground by mill and sieved to under 1 mm. The chemical and mineralogical compositions of raw slag were obtained by X-ray fluorescence spectrometry (XRF) (Shimadzu, XRF-1700) and X-ray diffraction (XRD) (Rigaku, RINT-2500), respectively (Table 1). Raw slag was mainly composed of CaO (42.9%), SiO_2 (34.5%), and Al_2O_3 (13.7%) in the form of amorphous phases. Other oxides, such as MgO, SO_3, Fe_2O_3, TiO_2, K_2O, and MnO, occurred in smaller amounts.

2.2 Synthesis

The synthesis procedure, based on our previous studies (Wajima, et al., 2011), was shown in Figure 2. Ten grams of the slag was mixed with 16 g of NaOH powder and ground to obtain a homogeneous mixture. This mixture was then heated in a nickel crucible in an air atmosphere at 600 °C for 6 h. The resultant material was cooled to room temperature and ground again to

p-ISSN 1675-7939; e-ISSN 2289-4934

obtain the precursor. Six grams of the precursor was added to 20 mL of distilled water in a 50-mL polypropylene vessel and stirred with a magnetic stirrer (600 rpm) at room temperature for 6 h. After stirring, the slurry was filtered, washed with distilled water and dried in an oven overnight at 60 °C to obtain the final product. The product phases and morphologies were analyzed by XRD and a scanning electron microscope (SEM) (Hitachi, S-4500), respectively.

Table 1: Chemical composition of BF slag, fused precursor and the product

Oxide (wt. %)	BF slag	Fused precursor	Product	
			Raw product	After phosphate removal
CaO	42.9	21.8	62.4	48.0
SiO_2	34.5	11.8	20.9	16.6
Al_2O_3	13.7	5.1	8.6	4.8
MgO	6.1	1.9	3.2	
K_2O	0.3	0.2	0.1	
Fe_2O_3	0.6	0.7	0.7	
SO_3	1.1	0.1	0.1	
Na_2O		57.3	3.7	
P_2O_5				29.3

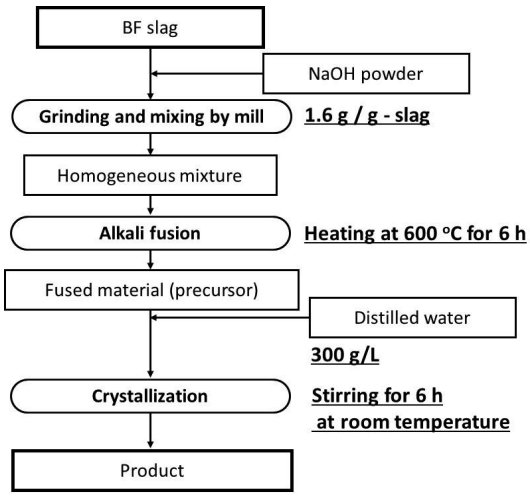

Figure 1: Flow Chart of the Experiment

2.3 Phosphate-removal

A batch mode operation was selected to evaluate the removal process. The effects of final pH (1 – 9), dosage (0 – 10 g/L), initial phosphate concentration (0 – 100 mmol/L), and contact time (0 – 24 h) were studied. The experiments were performed for sufficient durations to ensure equilibrium was reached. The pH of the initial solution and the supernatant was

p-ISSN 1675-7939; e-ISSN 2289-4934

measured by a pH meter (Horiba, D-53) and the concentrations of anions in the supernatant were determined using an ion chromatograph (IC) (ICS-3000, DIONEX Japan). The amounts of PO_4^{3-} removed, q (mmol/g), and percentages of anions removed, R (%), were calculated from the difference between the initial and final concentrations in the solution, as follows.

$$q = (C_0\text{-}C) \cdot V/w \quad (1)$$

$$R = (C_0\text{-}C)/C_0 \bullet 100 \quad (2)$$

where C_0 and C are the concentration of anions, including PO_4^{3-}, in initial and sampling solutions (mmol/L), respectively, V is the volume of the solution (L), and w is the weight of the sample (g).

The ability of the BF slag and the product to remove typical anions (F^-, Cl^-, Br^-, NO_3^-, SO_4^{2-}, and PO_4^{3-}) from aqueous solution was examined as follows. One-millimolar solutions were prepared with NaF, NaCl, NaBr, $NaNO_3$, Na_2SO_4, and $Na_2HPO_4 \bullet 12H_2O$. The sample (0.1 g) was added to 10 mL of 1 mM solution in a 50-mL centrifuge tube and shaken for 12 h using a reciprocal shaker. After shaking, the solution was centrifuged at 3000 rpm for 10 min. Concentrations of F^-, Cl^-, Br^-, NO_3^-, SO_4^{2-} and PO_4^{3-} in the supernatant were determined using an ion chromatograph. The amount of each anion removed was calculated from the difference between the initial and final solution concentrations.

The abilities of each product to remove phosphate in the presence of other anions (F^-, Cl^-, Br^-, NO_3^- and SO_4^{2-}) were examined. Each anion in the mixed solution was adjusted to 1 mM using NaF, NaCl, NaBr, $NaNO_3$, Na_2SO_4 and $NH_4H_2PO_4$, respectively. Then, 0.1 g of each product was added to 10 mL of the mixed solution in a 50-mL centrifuge tube and shaken for 12 h using a reciprocal shaker. After shaking, the solution was centrifuged at 3000 rpm for 10 min. The concentrations of each anion (F^-, Cl^-, Br^-, NO_3^-, SO_4^{2-} and PO_4^{3-}) in the supernatant were determined using the IC, and the amount of anion removed was calculated from the difference between the initial and final concentrations in the solution.

The effect of pH on phosphate removal was investigated using 100 mM $NH_4H_2PO_4$ with a final pH in the range of 3 – 12, by adjusting the initial solution pH within the range 1.5 – 3 using HCl. In each removal study, 0.1 g of sample was added to a 10-mL solution in 50-mL centrifuge tubes at room temperature and the tubes were shaken using a reciprocal shaker. After shaking for 12 h, the aqueous phase was separated from the solids by centrifugation. The pH of the initial solution and the supernatant were measured by a pH meter and the concentrations of PO_4^{3-} in the supernatant were determined to calculate the percentage of PO_4^{3-} removed at various solution pH values.

The effect of dosage on phosphate removal was determined using 1 mM $NH_4H_2PO_4$. The product (2 – 100 mg) was added to a 10-mL solution in a tube at room temperature and the tube was shaken for 12 h with a reciprocal shaker. After shaking, the aqueous phase was separated from the solids by centrifugation. The pH of the supernatant was measured using a pH meter and the concentration of phosphate in the supernatant was determined to calculate the phosphate removal percentage.

The effect of initial phosphate concentration on removal capacity of the product was determined. The product (0.1 g) was added to 10 mL of $NH_4H_2PO_4$ solution with

p-ISSN 1675-7939; e-ISSN 2289-4934

concentrations in the range 0 – 100 mmol/L in a tube at room temperature and the tube was shaken for 12 h with a reciprocal shaker. After shaking, the aqueous phase was separated from the solids by centrifugation. The pH of the supernatant was measured using a pH meter and the concentration of phosphate in the supernatant was determined to calculate phosphate removal percentage and the amount of phosphate removal.

To determine the removal rate of phosphate from aqueous solution, the product (0.1 g) was added to 10 mL of $NH_4H_2PO_4$ solution with a concentration of 10 mmol/L in a tube at room temperature, and the tube was shaken for 0 – 24 h with a reciprocal shaker. After shaking several times, the aqueous phase was separated from the solids by centrifugation. The pH of the supernatant was measured using a pH meter and the concentration of phosphate in the supernatant was determined to calculate the amount of phosphate removal. It should be noted that the pH of all solutions reached approximately pH 11 during the initial stage (below 30 min) and then remained almost constant.

3. RESULTS AND DISCUSSION

3.1 Synthesis of Adsorbent

Figure 2 shows XRD patterns of the (a) BF slag, (b) fused precursor and (c) product. The slag was composed of amorphous phases (Figure 2 (a)). After alkali fusion, soluble sodium salts, such as sodium silicate and sodium aluminate, appeared (Figure 2 (b)), and finally, the product, which included the crystalline phases, hydrocalumite and calcite, was synthesized (Figure 2 (c)).

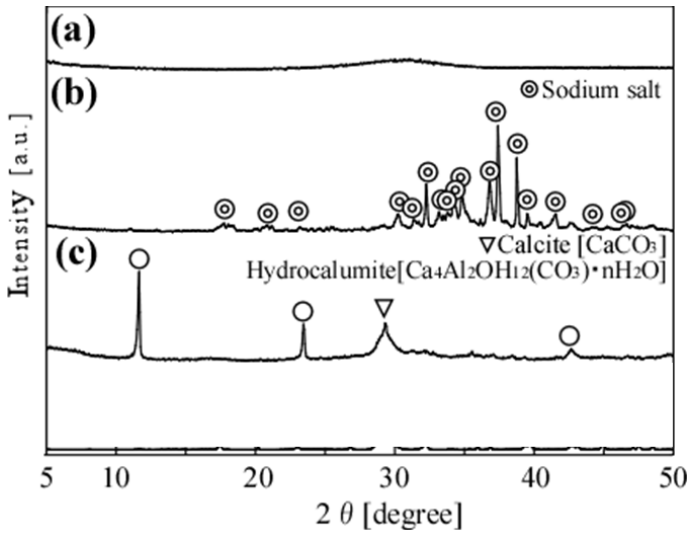

Figure 2: XRD Patterns of (a) BF Slag, (b) Precursor and (c) Product

Figure 3 shows SEM micrographs of (a) raw slag, (b) fused precursor and (c) product. Although the slag is composed of glass-like plates (Figure 3 (a)), the fused precursor consists of particles with a melted surface resulting from the formation of sodium salts by alkali fusion (Figure 3 (b)). After synthesis, the presences of thin regular hexagonal crystals of the hydrocalumite-type compound were confirmed in the product (Figure 3 (c)).

p-ISSN 1675-7939; e-ISSN 2289-4934

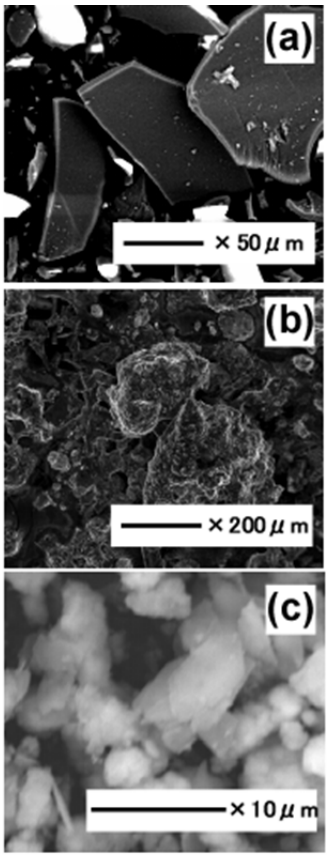

Figure 3: SEM Photographs of (a) BF Slag, (b) Precursor and (c) the Product

Table 1 shows the chemical compositions of the BF slag, fused precursor and product. As mentioned above, the slag mainly contained CaO (42.9 wt%), SiO_2 (34.5 wt%) and Al_2O_3 (13.7 wt%), and some minor elements. After alkali fusion, the obtained precursor contained higher amounts of Na_2O (57.3 wt%) and lower amounts of CaO (21.8 wt%), SiO_2 (11.8 wt%) and Al_2O_3 (5.1 wt%) than the raw slag, caused by the NaOH addition. After synthesis, the product mainly contained CaO (62.4 wt%), SiO_2 (20.9 wt%) and Al_2O_3 (8.6 wt%), arising from the calcite, hydrocalumite and amorphous calcium silicate in the product. It is noted that the mixture of slag (10 g) and NaOH powder (16 g) was converted into the precursor (24 g) to synthesize the product, including hydrocalumite (5.4 g). It is noted that specific surface areas of these materials are very low (< 20 m^2/g).

3.2 Removal Ability of Phosphate

Figure 4 shows the removal efficiencies of the slag and the product for certain anions from aqueous solutions. It is noted that the all supernatant pH values after the tests were approximately 12.6, regardless of the pH of the original solution. The product had high removal abilities for F^- (20.6%) and PO_4^{3-} (99.1%), while the removal efficiencies of raw slag for all anions were lower than 25%. The removal efficiencies of Cl^-, Br^-, SO_4^{2-} and NO_3^- (representative co-existing anions were much smaller than that of PO_4^{3-}. These results indicate that the removal of phosphate ions by the product from natural and wastewater would be unaffected by the presence of these other anions. Therefore, the product can be used as an adsorbent for water purification.

p-ISSN 1675-7939; e-ISSN 2289-4934

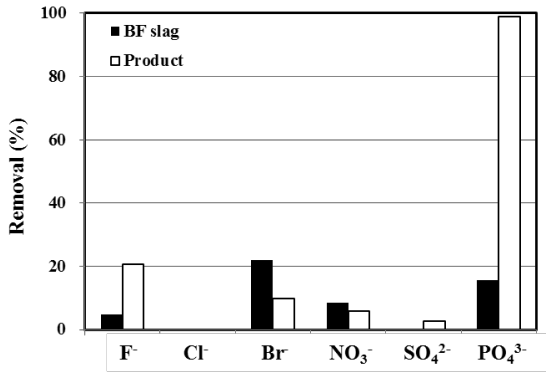

Figure 4: Removal Efficiencies for Anions by BF Slag and the Product in Each Anion Solution

Figure 5 shows the ability of the raw slag and product to remove anions from a mixed solution. It was noted that the pH of the solutions after experiments was constant at around pH 12.6. The raw slag showed higher removal abilities for PO_4^{3-} (38%) than those for other anions. Although other anions, F^-, Cl^-, Br^-, NO_3^- and SO_4^{2-}, were present in a mixed solution, the product indicates high removal efficiencies for PO_4^{3-} (100%), which is higher than that achieved using raw slag. The product thus has a high selective removal ability for PO_4^{3-}. It is also noted that the adsorbent has a higher removal ability for F^- than for the other anions.

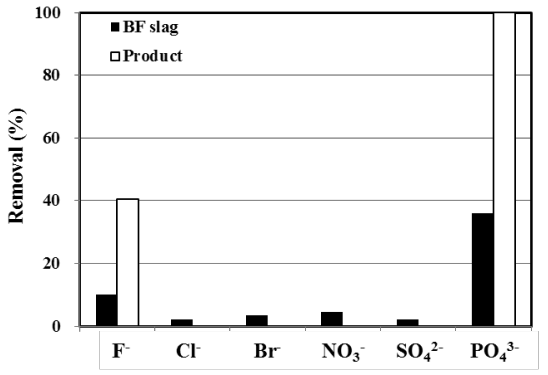

Figure 5: Removal Efficiencies for Anions by BF Slag and the Product in a Mixed Solution

The results are in good agreement with the results of Si-Fe-Mg and Si-Al-Mg mixed hydrous oxides, which are composed of three different group elements: the elements with cationic adsorption properties (Mg, Ca, Fe(II), etc.); those with anionic adsorption properties (Si, etc.); and those with amphoteric adsorption properties (Al, Fe(III), etc.) (Kuwabara, et al., 2007a; Kuwabara, et al., 2007b; Kuwabara, et al., 2010; Yanai, et al.,2010). The products obtained in this study were Si-Al-Ca mixed hydrous oxides, with similar compositions to the three different group elements and similar mineralogical properties. It is unclear why phosphate-selective adsorption occurs using these materials but materials with high contents of Mg or Ca display highly selective adsorption of phosphate and fluoride. It is known that HAP and MAP methods can remove phosphate selectively by the preferential formation of calcium phosphate and magnesium ammonium phosphate, with addition of a calcium or magnesium source (Ohtake, 2009). It is also known that fluoride ions in wastewater can be removed by the preferential formation of fluorite through addition of a calcium source such as calcite (Saha, 1993; Reardon & Wang, 2000). It is likely that these mixed hydrous oxides would supply

p-ISSN 1675-7939; e-ISSN 2289-4934

high contents of active Mg or Ca into the solution to react with phosphate or fluoride in solution.

The pH of the aqueous solution is an important for the phosphate removal process. Figure 6 shows the change in pH from the initial to the final equilibrium value. Solution equilibrium pH increased when the initial pH was acidic (1–5), indicating that the product is strongly basic.

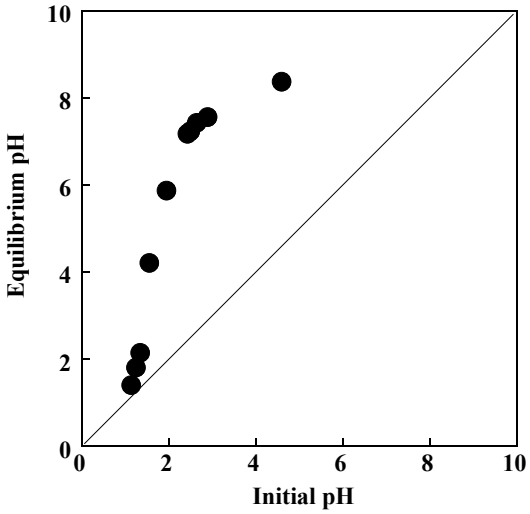

Figure 6: pH of the Solution before and after Phosphate Removal using the Product

The effect of pH on phosphate removal from solutions by the product is shown in Fig. 7. The percent of phosphate removed from solution increased with pH up to a value of 7 and then became almost constant (approximately 50%). This removal behaviour is good accordance with the results for calcined paper sludge (Wajima & Rakovan, 2013). An increase in pH of the solution becomes sufficient to form insoluble phosphate compounds by reaction between active Ca in the adsorbent and phosphate in the solution.

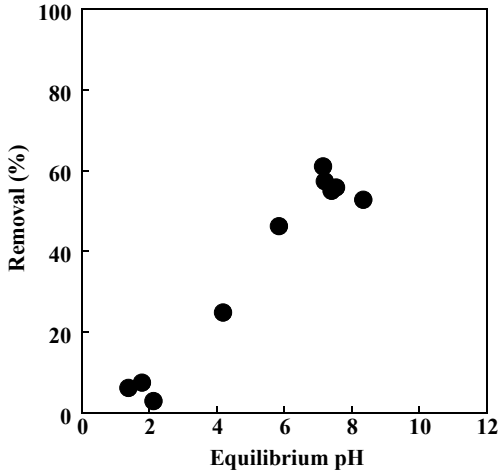

Figure 7: Phosphate Removal by the Product from Solution at different pH Values

p-ISSN 1675-7939; e-ISSN 2289-4934

Figure 8 illustrates the effect of dosage on phosphate removal by the product. As dosage increased to 1 g/L, removal of phosphate increased to approximately 100%, with phosphate removal becoming almost constant with further increases in dosage to 10 g/L. In Japan, the standard for phosphorous in effluents is < 16 mg/L-P (0.52 mmol/L), indicating 50% phosphate removal. The results indicate that a dosage exceeding 1 g/L is adequate for sufficient removal of phosphate from solution.

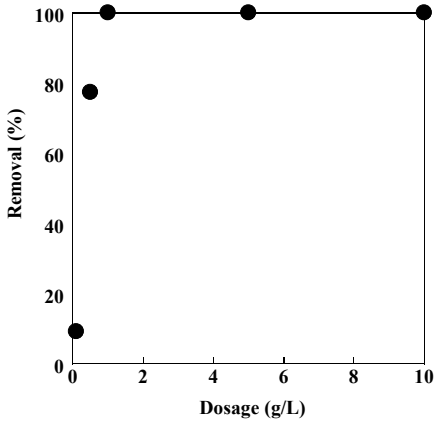

Figure 8: Effect of Dosage on Phosphate Removal using the Product

The effect of initial phosphate concentration on the phosphate removal ability of the product and equilibrium pH values of the solutions are shown in Figure 9. With the increase of the initial phosphate concentration, the removal percentage in a solution of up to 15 mM phosphate was 100%, followed by a gradual decrease in percentage removal above 15 mM concentration, and the equilibrium pH of the solution slightly decreased from 11 to 8.5. These results indicate that active sites for phosphate removal in the product are limited for the removal of phosphate ion in solutions with high initial phosphate concentrations. It is noted that the PO_4^{3-} removal efficiency of our product (100%) was better than that by calcite alone (94%) in a 1-mM PO_4^{3-} solution, because the content of active Ca, which reacts with phosphate ions to remove them from solution, would be higher in the product obtained via alkali fusion than that in calcite.

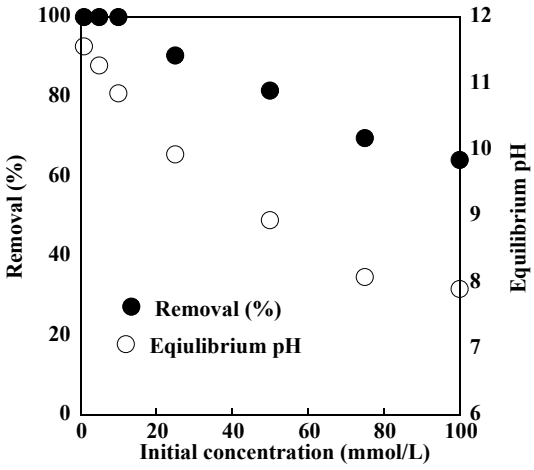

Figure 9: Phosphate Removal Percentage from Solution and the Equilibrium pH Values of the Solutions for Various Initial Phosphate Concentrations.

p-ISSN 1675-7939; e-ISSN 2289-4934

Figure 10 shows XRD patterns of the product after phosphate removal in $NH_4H_2PO_4$ solutions at (a) 10 mM, (b) 50 mM and (c) 100 mM. In the case of 10 mM, the peaks of hydrocalumite [$Ca_4Al_2O_6(OH)_2 \cdot 11H_2O$] diminished and those of calcite [$CaCO_3$] remain in the product and small peaks of hydroxyapatite [$Ca_5(PO_4)_3(OH)$] appear. In the case of 50 mM, the peaks of hydrocalumite diminish and the heights of calcite peaks decrease more than those in 10 mM, while the heights of hydroxyapatite peaks increase more than for 10 mM. Furthermore, in the case of 100 mM, the hydrocalumite and calcite peaks diminish, and brushite [$CaHPO_4 \cdot 2H_2O$] appears. This is in good agreement with the results for $CaO\text{-}SiO_2\text{-}Al_2O_3$ (C-A-S-H) gel (Okada, et al., 2007). It was also reported that crystal growth of hydroxyapatite occurs on the hydrocalumite surfaces by reaction between calcium ions eluted from hydrocalumite and the phosphate ions in solution (Watanabe, et al., 2010). The products from BF slag, including CaO, SiO_2 and Al_2O_3, would contain not only the crystal phases, calcite and hydrocalumite, but also an amorphous, gel-like calcium aluminum silicate hydrate (C-A-S-H) product. The mechanism of phosphate sorption onto the product can be explained in terms of the precipitation of calcium phosphates, caused by the dissolution of calcium from the product (gel, hydrocalumite and calcite) with phosphate ions in the solution. The order of dissolution would be C-A-S-H gel > hydrocalumite > calcite, and the dissolution would increase with increasing phosphate concentration in the solution. On the other hand, the releases of silicon and aluminium ions into the solution by the dissolution of the C-A-S-H gel and hydrocalumite occur, and these ions buffer the pH of solution (Iler, 1979; Watanabe, et al., 2010). Therefore, with increasing phosphate concentrations in solution, the amount of phosphate removed increases and the pH values of the solution, after removal tests, decrease, as shown in Figure 9.

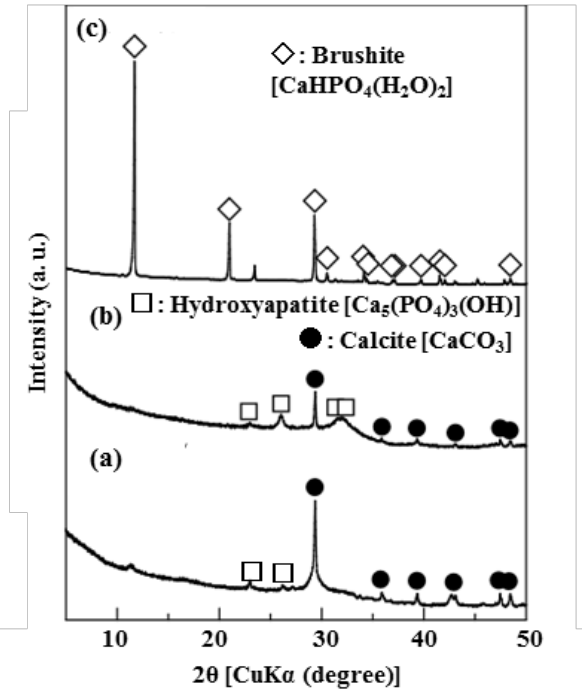

Figure 10: XRD Patterns of the Product after Phoshpate Removal from Solutions with Initially (a) 10 mM, (b) 50 mM, (c) 100 mM Phosphate.

Table 1 shows the chemical compositions of the product before and after phosphate removal experiment using 100 mM phosphate solution. After phosphate removal, the product indicates

p-ISSN 1675-7939; e-ISSN 2289-4934

higher phosphate content than typical phosphate ore rocks, which means that the product after phosphate removal can be used as phosphate resources.

Figure 11 shows the amount of PO_4^{3-} removed using the product. As the equilibrium concentration of phosphate increases, the amount of PO_4^{3-} adsorbed by the product increases at low phosphate concentrations, and then gradually increases.

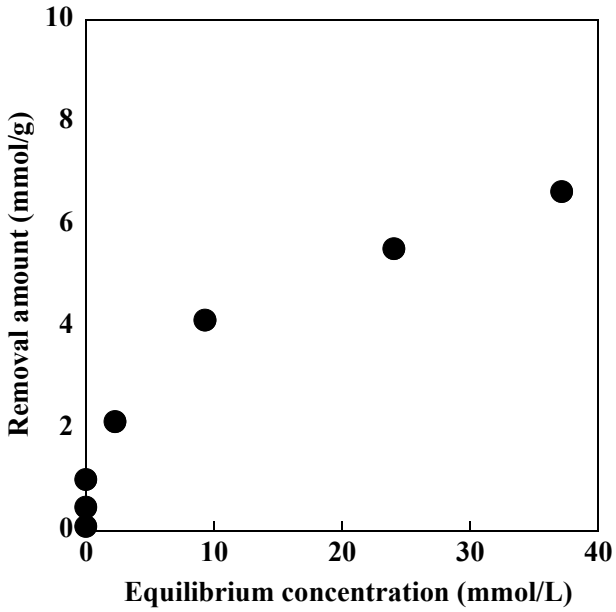

Figure 11: Amounts of PO_4^{3-} Removed using the Product

The phosphate removal behavior of the product is determined by the Langmuir and Freundlich isotherm models. The linear form of the Langmuir model is given by

$$C_e/q_e = 1/(q_{max} \bullet K_L) + C_e/q_{max} \quad (3)$$

where q_e is phosphate concentration adsorbed to the product at equilibrium (mmol of phosphate ion / g of the adsorbent); q_{max} (mmol/g) and K_L (L/mmol) are Langmuir constants related to the maximum adsorption capacity and adsorption energy (equilibrium adsorption constant), respectively. These constants are found from the slope and intercept of a C_e / q_e vs. C_e linear plot, whereby q_{max} = 1 / slope and K_L = slope / intercept.

The linear form of the Freundlich model is given by:

$$\ln(q_e) = \ln(K_F) + (1/n) \bullet \ln(C_e) \quad (4)$$

where K_F and n are the Freundlich constants determined from the slope and intercept of plotting $\ln(q_e)$ vs. $\ln(C_e)$.

The values of the Langmuir and Freundlich constants and regression coefficients for phosphate removal are given in Table 2. In the case of the Langmuir model, our experimental results give a correlation regression coefficient (R^2) equal to 0.988, which is the measure of goodness-of-fit and the general empirical formula of the Langmuir model by C_e / q_e =

p-ISSN 1675-7939; e-ISSN 2289-4934

0.1304C_e +0.9512. In the case of the Freundlich model, we observed that the empirical formula of this model was found to be $\ln(q_e)=0.4007\ln(C_e) + 0.4562$ with R^2 value equal to 0.992. It can be seen that the Freundlich model provides a better fit than the Langmuir model, because the former has a higher correlation regression coefficient than the latter. The maximum adsorption capacity of the product for PO_4^{3-} calculated from the Langmuir model is 7.67 mmol/g, which is higher than other adsorbents reported previously, as shown in Table 3.

Table 2: Values of Langumiur and Freundlich Constants and Regression Coefficient for Phosphate Removal

Langmuir Constant			Freundlich constant		
q_{max}	K_L	R^2	n	K_F	R^2
7.67	0.14	0.988	1.58	2.50	0.992

Table 3: Maximum Phosphate Sorption Capacities of Adsoebents reported in the Literatures

Adsorbent	q_{max} (mmol/g)	References
Steel-making slag	6.96	Jha, et al., 2008
Calcined alunite	3.81	Özcar, 2003
Amorphous calcium silicate	1.9	Southam, et al., 2004
Zr(IV)-loaded orange waste gel	1.84	Biswas, et al., 2008
Hydortalcite	1.53	Kuzawa, et al., 2006
Amorphous Al hydroxide	1.3	Lookman, et al., 1997
Amorphous hydrous iron oxide gel	0.95	Parfitt, et al., 1975
Red mad	0.75	Pradhan, et al., 1998
Coal fly ash	0.75	Pengthamkeerati, et al., 2008
Crystalline blast furnace slag	0.61	Kostura, et al., 2005
Zirconium ferrite	0.42	Biswas, et al., 2008

Figure 12 illustrates phosphate removal by the product during reaction. The slopes of the lines joining the data points in the figure reflect the removal rates. The amount of phosphate removed increased rapidly and reached equilibrium after 60 min. In previous studies, several adsorbents were used for phosphate removal, with 200 – 300 min being reported as the equilibrium adsorption time (Biswas, et al., 2008; Jutidamrongphan, et al., 2012). Short times for phosphate removal are favored to minimize energy consumption; therefore, the product can be considered efficient for phosphate removal because of its short removal time.

The kinetics results obtained from Figure 12 were analyzed using different kinetics models, such as the Lagergen pseudo first-order and pseudo second-order models (Wajima, et al., 2009). The Lagergen pseudo first-order model is given by

p-ISSN 1675-7939; e-ISSN 2289-4934

$$\ln(q_e - q_t) = \ln(q_e) - k_1 \cdot t \quad (5)$$

where q_t is the phosphate amount on the adsorbent at any time (mmol/g) and k_1 is the adsorption rate constant (min^{-1}). A liner plot of $\ln(q_e - q_t)$ against t gives the slope = k_1 and intercept = $\ln(q_e)$.The equation that describes the pseudo second-order model is given in the following linear form:

$$t/q_t = 1/(k_2 \cdot q_e^2) + t/q_e \quad (6)$$

where k_2 is the adsorption rate constant (g/mmol-min). k_2 and q_e are found from the intercept and slope of t/q_t vs. t linear plot, so that q_e = 1 /slope and k_2 = slope^2 / intercept. The rate constants of the pseudo first-order model, k_1, and pseudo second-order model, k_2, for phosphate removal were determined from Figure 12. These values are shown in Table 4. The degree of goodness of the linear fits of these kinetic models can be judged from the value of the coefficient of determination of the plots, which can also be regarded as the criterion in the determination of adequacy of a kinetic model. Figure 12 shows that the coefficients of determination values are 0.956 and 0.999, respectively, so the phosphate removal by the product can be regarded to follow a pseudo second-order rather than a pseudo first-order model.

Table 4: Kinetics Parameters for Phosphate Removal by the Product and Regression Coefficient

Pseudo-first-order kinetics model			Pseudo-second-order kinetics model		
$q_{e,1}$	k_1	R^2	$q_{e,2}$	k_2	R^2
0.19	0.18	0.956	1.04	4.97	0.999

4. CONCLUSION

BF slag was converted into phosphate adsorbents using alkali fusion, and the abilities of the product to remove phosphate ions were investigated. The slag was transformed into a precursor with reactive phases through alkali fusion, and the product, containing hydrocalumite and calcite, was then synthesized by stirring in distilled water at room temperature. The product has a higher removal ability for F^- and PO_4^{3-} than that of raw slag, and removed negligible amounts of anions typically present in natural and waste water, such as Cl^-, Br^-, NO_3^- and SO_4^{2-}. The selective removal of PO_4^{3-} by the product was especially high in a mixed solution containing F^-, Cl^-, Br^-, NO_3^- and SO_4^{2-}. The product removed phosphate from aqueous solutions by forming the calcium phosphate minerals, hydroxyapatite and brushite, and can contain high phosphate to use as phosphate resources. The equilibrium data for PO_4^{3-} removal fitted the Freundlich isotherm model slightly better than the Langmuir model, and the maximum adsorption capacity of the product calculated from the Langmuir model was higher than other adsorbents prepared from waste reported previously. The kinetics of phosphate removal from aqueous solution follows a pseudo second-order model rather than a pseudo first-order model. The results show that a product with excellent PO_4^{3-} removal abilities for reducing environmental pollution that causes eutrophication in wastewater can be synthesized from BF slag using alkali fusion.

p-ISSN 1675-7939; e-ISSN 2289-4934

5. ACKNOWLEDGEMENT

This research was supported by a Research Promotion Grant from the Iron and Steel Insitute of Japan.

REFERENCES

Biswas, B. K., Inoue, K., Ghimire, K. N., Harada, H., Ohoto, K., & Kawakita, H. (2008). Removal and recovery of phosphorus from water by means of adsorption onto orange waste gel loaded with zirconium, *Bioresource Technology,* 99: 8685-8690.

Can, M. Y., & Yildiz, E. (2006). Phosphate Removal from Water by Fly Ash: Factorial Experimental Design, *Journal of Hazardous Materials*, B135, 165-170.

Chang-jun,ch L., Yan-zhong, L., Zhao-kun, L., Zhao-yang, C., Zhong-guo, Z., & Zhi-ping J.(2007). Adsorption Removal of Phosphate from Aqueous Solution by Active Red Mud, *Journal of Environmental Sciences*, 19, 1166-1170.

Fujiwara, M. (2003). *Bulletin of The Iron and Steel Institute of Japan*, 8, 883-889.

Hoon, J., & Kang, S. (2002). Phosphorus Removal using Cow Bone in Hydroxyapatite Crystallization, *Water Research*, 36, 1324-1330.

Huang, S.-H., & Chiswell, B. (2000). Phosphate Removal from Wastewater using Spent Alum Sludge, *Water Science and Technology*, 42, 295-300.

Iler, R. K. (1979). *The Chemistry of Silica*, Wiley-Interscience, New York.

Jha, V. K., Kameshima, Y., Nakajima, A., & Okada, K. (2008). Utilization of Steel-making Slag for the Uptake of Ammonium and Phosphate Ions from Aqueous Solution, *Journal of Hazardous Materials*, 156, 156-162.

Johansson, L., & Gustafsson, J. P. (2000). Phosphate Removal using Blast Furnace Slags and Opoka-Mechanisms, *Water Research*, 34, 259-265.

Jutidamrongphan, W., Park, K. Y., Dockko, S., Choi, J. W., & Lee, S. H. (2012). High Removal of Phosphate from Wastewater using Silica Sulfate, *Environmental Chemistry Letters*, 10: 21-28.

Kostura, B., Kulveitova, H., & Lesko, J. (2005). Blast furnace slags as sorbents of phosphate from water solutions, *Water Research*, 39: 1795-1802.

Kuroki, T., Uchida, Y., Takizawa, H., & Morita, K. (2007). Effects of 28 GHz/2.45 GHz Microwave Irradiation on the Crystallization of Blast Furnace Slag, *ISIJ International*, 47, 592-595.

Kuwabara, T., Arakawa, K., Sato, T., & Onodera, Y. (2007a). Synthesis and Characterization of Si-Fe-Mg Mixed Hydrous Oxides as Harmful lons Removal Materials, *Journal of the Society of Inorganic Materials Japan*, 14, 104-113.

p-ISSN 1675-7939; e-ISSN 2289-4934

Kuwabara, T., Arakawa, K., Sato, T., & Onodera, Y. (2007b). Adsorption Properties of Synthetic Si-Fe-Mg Mixed Hydrous Oxides, *Journal of Japan Society on Water Environment*, 30, 133-138.

Kuwabara, T., Kikuchi, K., Sato, T., & Onodera, Y. (2010). Synthesis of Si-Al-Mg Mixed Hydrous Oxides and Their Ion Adsorption Behavior, *Journal of the Society of Inorganic Materials Japan*, 17, 81-88.

Kuzawa, K., Jung, Y.-J., Kiso, Y., Yamada, T., Nagai, M., & Lee, T.-G. (2006). Phosphate Removal and Recovery with a Synthetic Hydrotalcite as an Adsorbent, *Chemoshere*, 62: 45-52.

Lee, J.-H., Yubata, K., Hayashi, A., & Morita, K. (2003). Characterization of Fibrous Particles in Blast Furnace Slag Quenched by Water-spray, *ISIJ International*, 43, 2073-2075.

Lookman, R., Grobet, P., Merckx, R., & Van Riemsdijk, W. H. (1997). Application of P and Al MAS NMR for Phosphate Speciation Studies in Soil and Aluminium Hydroxides: Promises and Constrants, *Geoderma*, 80, 369-388.

Lu, S. G., Bai, S.Q., Zhu, L., & Shan, H. D. (2009). Removal Mechanism of Phosphate from Aqueous Solution by Fly Ash, *Journal of Hazardous Materials*, 161, 95-101.

Miki, T., Futatsuka, T., Shitogiden, K., Nagasaka, T., & Hino, M. (2004). Dissolution Behavior of Environmentally Regulated Elements from Steelmaking Slag into Seawater, *ISIJ International*, 44, 762-769.

Namasivayam, C., Sakoda, A., & Suzuki, M. (2005). Removal of Phosphate by Adsorption onto Oyster Shell Powder –Kinetics Studies-, *Journal of Chemical Technology and Biotechnology*, 80, 356-358.

Ohtake, H. (2009). *Recovery of Phosphorous Resources and its Utilization*, Science & Technology, Tokyo.

Okada, K., Ono, Y., Kameshima, Y., Nakajima, A., & MacKenzie, K. J. D. (2007). Simultaneous Uptake of Ammonium and Phosphate Ions by Compounds Prepared from Paper Sludge Ash, *Journal of Hazardous Materials*, 141, 622-629.

Özacar, M. (2003). Adsorption of Phosphate from Aqueous Solution onto Alunite, *Chemosphere*,.51, 321-327.

Ozdemir, I., & Yilmaz, S. (2007). Processing of Unglazed Ceramic Tiles from Blast Furnace Slag, *Journal of Materials Processing Technology*, 183, 13-17.

Parfitt, L., Atkinson, J., & Smart, C. S. (1975). The Mechanism of Phosphate Fixation by Iron Oxides, *Soil Science Society of America, Proceedings*, 39, 837-841.

Pengthamkeerati, P., Satapanajaru, T., & Chularuengoaksorn, P. (2008). Chemical Modification of Coal Fly Ash for the Removal of Phosphate from Aqueous Solution, *Fuel*, 87, 2469-2476.

p-ISSN 1675-7939; e-ISSN 2289-4934

Pradhan, J., Das, J., Das, S., & Thakur, R. S. (1998). Adsorption of Phosphate from Aqueous Solution using Red Mud, *Journal of Colloid and Interface Science*, 204, 169-172

Reardon, E. J., & Wang, Y. (2000). A Limestone Reactor for Fluoride Removal from Wastewaters, *Environmental Science and Technology*, 34, 3247-3253.

Saha, S. (1993). Treatment of aqueous effluent for fluoride removal, *Water Research*, 27: 1347-1350.

Savastona, H., Agopyan, V., Nolasco, A. M., & Pimentel, L. (1999). Plant Fibre Reinforced Cement Components for Roofing, *Construction and Building Materials*,13, 433-438.

Southam, D. C., Lewis, T. W., McFarlane, A. J., & Johnston, J. H. (2004). Amorphous Calcium Silicate as a Chemisorbent for Phosphate, *Current Applied Physics*, 4, 355-358.

Ugurlu, A., & Salman, B. (1998). Phosphorous Removal by Fly Ash, *Environment International*, 24, 911-918.

Wajima, T., Oya, K., Shibayama, A., Sugawara, K., & Munakata, K. (2011). Synthesis of Hydrocalumite-like Adsorbent from Blast Furnace Slag using Alkali Fusion, *ISIJ International*, 51, 1179-1184.

Wajima, T., & Rakovan, J. F. (2013). Removal Behavior of Phosphate from Aqueous Solution by Calcined Paper Sludge, *Colloids and Surfaces A*, 435, 132-138.

Wajima, T., Umeta, Y., Narita, S., & Sugawara, K. (2009). Adsorption Behavior of Fluoride Ions using a Titanium Hydroxide-derived Adsorbent, *Desalination*, 249, 323-330.

Watanabe, Y., Ikoma, T., Yamada, H., Stevens, G. W., Moriyoshi, Y., Tanaka, J., & Komatsu, Y. (2010). Formation of Hydroxyapatite Nanocrystals on the surface of Ca-Al Layered Double Hydroxide, *Journal of American Ceramic Society*, 93, 1195-1200.

Xiong, J. B., & Mahmood, Q. (2010).Adsorption Removal of Phosphate from Aqueous Media by Peat. *Desalination*, 259, 59-64.

Xu, X., Gao, B.-Y., Yue, Q.-Y., & Zhong, Q.-Q. (2010). Preparation of Agricultural By-product Based Anion Exchanger and its Utilization for Nitorgen and Phosphate Removal, *Bioresource Technology*, 101, 8558-8564.

Yabuta, K., Tozawa, H., & Takahashi, T. (2004). New Applications of Iron and Steelmaking Slag Contributing to a Recycling-oriented Society, *JFE Techical Report*, 8, 17-23.

Yanai, K., Kuwabara, T., Oshima, H., & Sato, T. (2010). Study on the Fluoride Removal from Hot Spring Waste Water Using Si-Al-Mg Mixed Hydrous Oxide, *Journal of the Clay Science Society of Japan*, 49, 128-135.

Yeom, S. H., & Jung, K.-Y. (2009). Recycling Wasted Scallop Shell as an Adsorbent for the Removal of Phosphate, *Journal of Industrial and Engineering Chemistry*, 15, 40-44.

p-ISSN 1675-7939; e-ISSN 2289-4934

Zeng, L., Li, X., & Liu, J. (2004). Adsorptive Removal of Phosphate from Aqueous Solutions using Iron Oxide Tailings, *Water Research*, 38, 1318-1326.

p-ISSN 1675-7939; e-ISSN 2289-4934